DETERMINATION OF AN INERTIAL CAVITATION THRESHOLD OF THE DEFINITY® MICROBUBBLE ULTRASOUND CONTRAST AGENT

Briarcliff Manor High School

444 Pleasantville Road

Briarcliff Manor, NY

10510

I. INTRODUCTION

More than 25 years ago, it was reported that ultrasound (US) might enhance the fibrinolytic process. This process entails a fibrin clot, the product of coagulation, being broken down, whose main enzyme, plasmin, cuts the fibrin mesh at various places, leading to the production of circulating fragments that are cleared by other proteinases or by the kidney and liver. Between the 1980's and present day, many studies have explored and confirmed the fibrinolytic effect of US (Trubestein G., 1976). Although the use of US has been shown to be beneficial in enhancing the fibrinolysis process, it may also be harmful to other biological tissue in other circumstances. For example, US might be detrimental to already injured tissue (Barnett SB, et al., 1997). Accordingly, the same mechanisms by which US may be potentially harmful are in fact similar to those described in connection with US enhanced fibrinolysis (Barnett SB, et al., 1997). However it is still unclear as to how US essentially contributes to the profibrinolytic mechanism.

Ultrasound Contrast Agents (UCA) are traditionally used for contrast enhancement of blood vessels because UCA's have a high degree of echogenicity, which is the ability of an object to reflect the ultrasound waves. The echogenicity difference between the gas in the microbubbles and the soft tissue surroundings of the body is immense. Thus, ultrasonic imaging using microbubble contrast agents enhances the ultrasound backscatter, or reflection of the ultrasound waves, to produce a unique sonogram with increased contrast due to the high echogenicity difference. Several imaging techniques were later developed using linear and nonlinear microbubble responses to measure blood perfusion, blood volume or blood velocity rates in tissue. For example, a high-intensity ultrasonic burst applied to a targeted area purposefully reduces the UCA concentration and the contrast enhancement can be used to measure blood volume and flow rates by monitoring the rate at which the echogenicity returns due to

the UCAs being reintroduced to that tissue region.

Recently, several studies have explored the potential of therapeutic angiogenesis or ateriogenesis using US-UCA interaction. Consequently, in the search for clinically relevant applications, researchers have examined the potential of cellular (Assmus et al., 2002; Iba et al., 2002; Iwaguro et al., 2002), molecular (Ito et al., 1997; van Royen et al., 2002) and genetic (Grines et al., 2003; Hiasa et al., 2004) interventions for therapeutic neovascularization. For example, patients with occlusive vascular diseases, such as atherosclerosis and diabetes, who are ineligible for surgical revascularization, may benefit from the targeted stimulation of neovascularization (Schirmer and Royen, 2004) (Chapell et al., 2005).

As seen in studies such as Song et al. (2002a), the application of low-frequency US to intravascular UCAs creates small capillary ruptures. In this study as well as similar studies such as Skyba et al. (1998) and Chapell et al. (2005) the researchers hoped that the small capillary ruptures would elicit neovascularization though an in vivo wound healing mechanism. This healing mechanism is most likely a result of the recruitment of cells known to be involved in neovascularization. This group of specialized cells includes the inflammatory cells that play a known key role in the vascular remodeling responses (Leibovich et al. 1987; Scholz et al. 2000; Sunderkotter et al. 1994). The inflammation response following US-UCA treatment may include the recruitment of monocytes and macrophages to the sites of US-UCA interaction and destruction, which is thought to initiate and regulate neovascularization (Skyba et al. 1998). It has also been speculated that US-UCA interaction can elicit neovascularization through changes in hemodynamics and microvessel permeability (Chapell et al, 2005). Capillaries disrupted by US-UCA interactions may become hyper-permeable, enabling extravasation of blood components and plasma, which in turn could trigger neovascularization. The

exact mechanism through which US-UCA interaction elicits a neovascular response has not been characterized.

Presently, US and UCA interaction has facilitated successful transfer of genetic material to numerous tissues including the myocardium (Bekeredjian et al. 2003; Kondo et al. 2004; Shohet et al. 2000); arterial vessels (Porter et al. 2001; Taniyama et al. 2002a); the nervous system (Shimamura et al. 2004); and skeletal muscle (Song et al.(2002b). Other studies have explored the possibility of applying therapeutic US with the aid of UCA to the opening of the blood brain barrier, targeted drug and gene delivery (Hynynen et al 2001), detection and lysis of blood clots (Luo et al, 1998, Porter et al, 1996), neovascularization (Song et al. 2002a), and sonoporation (Fechheimer et al, 1986). However, all of the aforementioned techniques require that UCA collapse thresholds be known in order to assess whether or not UCA collapse causes the effect. Because the aforementioned applications all rely upon the collapse response of the excited microbubbles in vivo, the knowledge of the collapse threshold remains pertinent and necessary.

A. Objectives and Hypothesis

This study aims to determine an inertial cavitation (IC) threshold estimate (also known as a collapse threshold estimate) by inspecting the data for the lowest peak rarefactional pressure where microbubble collapses were present for the contrast agent Definity®. In order to obtain data for inspecting, this study will take advantage of a passive cavitation detetction system (PCD). Instead of analyzing signals received during acoustic excitation, the PCD will record broadband emissions occuring between 1 and 5 us after excitation were identified. This study also aims to facilitate all

research being done ~~to~~ by establishing an accepted threshold level for collapse; an integral part in inducing therapeutic responses. This study's objective is, therefore, to test whether in vitro determined ultrasound contrast agent collapse thresholds are the same as those determined under in vivo conditions using an animal-based angiogenesis response based on type of contrast agent, frequencies used, pulse duration (PD) and pressure level (peak rarefactional pressure).

i. Hypothesis

$H_1 - X_a \leq X_b$ (*In vitro* determined ultrasound contrast agent collapse thresholds (X_a) are lower or equal to those thresholds determined under *in vivo* conditions (X_b) using an animal-based angiogenesis response)

$H_0 - X_a > X_b$ (*In vitro* determined ultrasound contrast agent collapse thresholds are higher to those thresholds determined under *in vivo* conditions using an animal-bases angiogenesis response)

II. PROCEDURES AND METHODS

A. Introduction To Methods

In the search to estimate the collapse threshold for the UCA Definity®, this study made us of a passive cavitation detector with confocal transducers operated with center frequencies of 0.9, 2.8, 4.6, 7.1 *MHz* and tone bursts, with a pulse duration of 3,5 or 7 cycles. In a water tank, the UCAs were exposed to each pressure level and the excitation response was recorded using a 13-MHz receiving transducer. For all pressure levels, 500 samples were collected and a spectrogram was created from the ten highest amplitude waveforms per sample. These spectrograms were then classified into 5 distinct categories based on a characteristic broadband signal emitted from the excited bubble: Noise, Oscillation, Collapse, Multiple Bubble and Unidentified.

C. Contrast Agents

The FDA-approved contrast agent Definity® (Bristol-Myers Squibb Medical Imaging, N. Billerica, MA) was used for all experiments. Definity® is comprised of lipid-coated microspheres filled with octafluoropropane gas (C_3F_8). Each vial of Definity® contains a maximum concentration of 1.2 x 10^10 microbubbles/mL. Before each use, the Definity® vials were activated using Vialmix®**(**Bristol-Myers Squibb Medical Imaging Inc, N. Billerica, MA**)**. The maximum diameter of a single microbubble is less than 20 µm. However, approximately 98% of the bubbles have a diameter of less than 10 µm. The microspheres contained in the vials have a mean diameter of 1.1–3.3 µm. (Definity®, Bristol-Myers Squibb Medical Imaging, N. Billerica, MA)

D. Exposure Apparatus (Fig. 1)

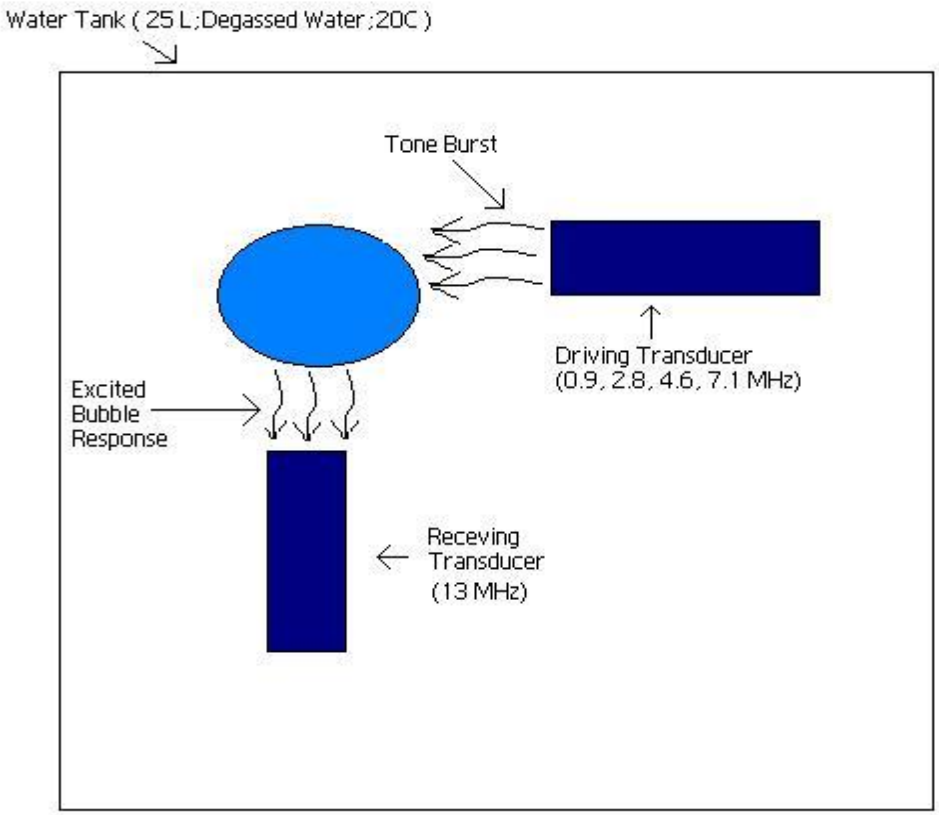

Fig 1. Experimental setup of the Passive Cavitation Detector(PCD)

The field to which the UCAs were exposed was generated using four separate driving transducers. The confocal transducers operated with center frequencies of 0.9, 2.8, 4.6, 7.1 *MHz*. The exposure occurred in a 50.5-cm long x 25.5-cm wide x 30-cm high water tank. The tank was filled with 25 ± 0.6 L of degassed water at 20C. Tone bursts with a pulse duration of 3,5 or 7 cycles and center frequencies of 0.9, 2.8, 4.6 or 7.1 *MHz* were generated by a RITEC RAM5000 pulser-reciever. (RITEC, Warwick, RI). The pulse repetition frequency was set to 10 Hz and the pulse phase was set to 180° for all experiments. A focused 13-MHz receive transducer was positioned in a 90° angle to the 0.9 and 7.1 *MHz* transducers. However, the receive transducer was positioned at a 45° angle to the 2.8 and 4.6 Mhz. These configurations were set in order to allow the receiving transducer's focal region to be within the confocal volume of the driving transducer. The received signal from the microbubbles was amplified (44 dB), digitized (12-bit, 200 MS/s, Strategic Test digitizing board UF 3025, Cambridge, MA) and then saved to a PC for post-processing using Matlab® (The Math Works, Inc., MA).

E. Data acquisition

A 1-mL syringe was used to inject a solution of 0.1-mL Definity ® into the exposure apparatus. The solution with a concentration of 25 x 10^8 UCAs yielded a concentration of 10 microbubbles / μL. These concentrations allowed approximately 1 microbubble at a time in the focal zone of the Passive Cavitation Detector (PCD). The water in the tank was stirred gently using a magnetic stirrer in order to maintain an even distribution of microbubbles for all experiments. For each pulse duration (PD) (3, 5 and 7 cycles) five hundred waveforms were acquired using the 13 *MHz* receiving transducer. All trials were executed in the same way except for changing the driving transducer's frequency (0.9, 2.8, 4.6 and

7.1 *MHz*). 10,500 samples were collected per each pulse duration, resulting in a total of 126,000 samples collected.

F. Data Processing and Classification

All waveforms were sorted from the highest to the lowest amplitude. The offset of each waveform was removed by subtracting the mean value and then the waveforms were filtered though a bandpass (FIR, 1 -25 *MHz* passband) to reduce signals that occurred outside the impulse response of the receiving transducer. For all pressure levels, a spectrogram was created from the ten highest amplitude waveforms. All spectrograms were generated by means of the implemented Matlab® function (spectrogram; 128 point Hanning window, 126 point overlap, 8192 point fft).

After processing, all data were classified into 5 distinct categories according to Noise, Oscillation, Collapse, Multiple Bubbles and Unidentified.

i. Noise

Despite the high likelihood that only one microbubble would be in the focal zone at a given time, there were cases in which no microbubbles were in that volume. This situation resulted in no microbubble generated echoes; all that can be seen is broadband noise. (Fig 2)

Fig 2. Classification of the Signal "Noise"

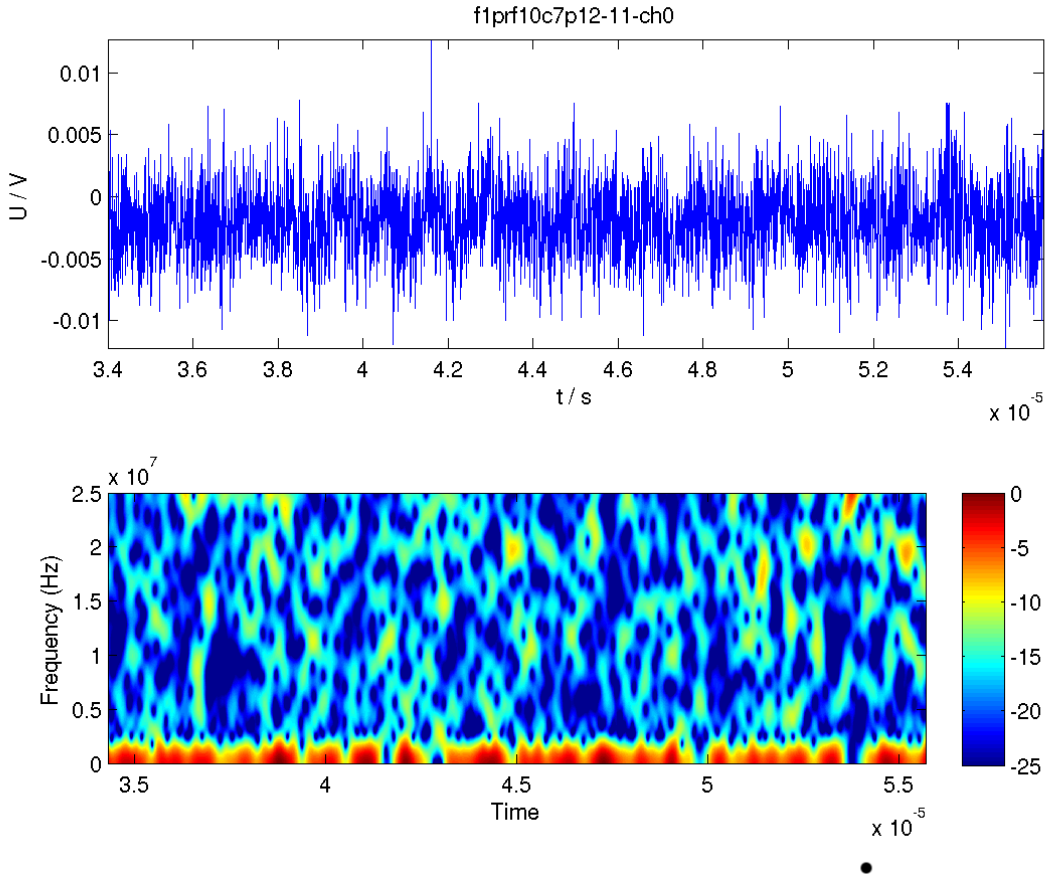

Fig 2. Representative waveform of the class "Noise". A .9-MHz 7-Cycle sinusoidal tone burst was used to excite this bubble

Figure is hiding the text

ii. Oscillation

Figure 3 shows a PCD waveform that can be classified under the class of Oscillation. The waveform between 44 and 47 µs corresponds to the scattered microbubble echo. What is visible in the spectrogram could have been generated by the nonlinear bubble dynamics and nonlinear propagation of the exciting pulse and scattered echo. No acoustic emissions were present after the termination of the driving pulse.

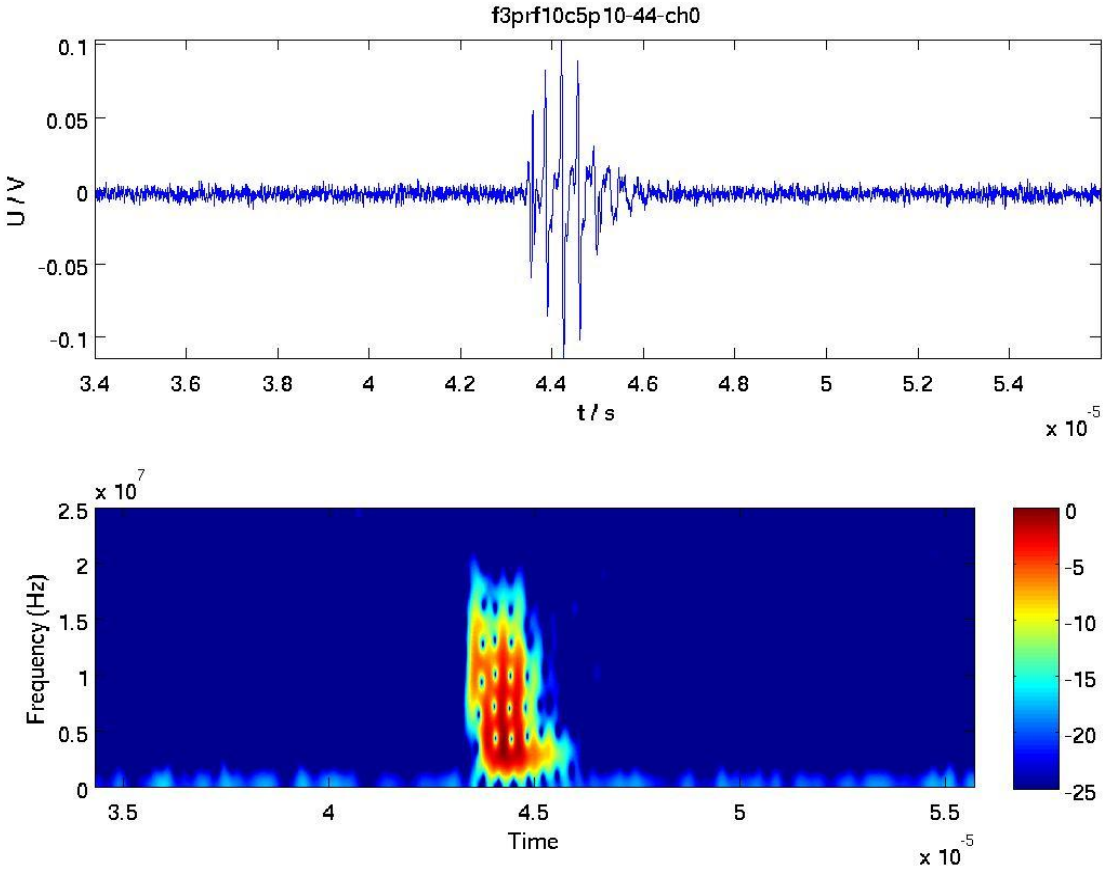

Fig 3. Classification of the Signal "Oscillation"

Fig 3. Representative waveform of the class "Oscillation". A 2.8-MHz 3-Cycle sinusoidal tone burst was used to excite this bubble

iii. Collapse

Figure 4 shows a single microbubble that was classified as Collapsed. The response shown between 44 and 47 µs looks similar to a waveform classified as Oscillation, however, the factor that characterizes this spectrogram as Collapse as opposes to Oscillation is apparent within the response between 435 and 450 µs. The post-principal response indicated that inertial cavitation occurred and a free bubble formed. The second response is thus an indication that a free bubble also sent a rebound single to the receiving transducer and thus a collapse occurred.

Fig 4. Classification of the Signal "Collapse"

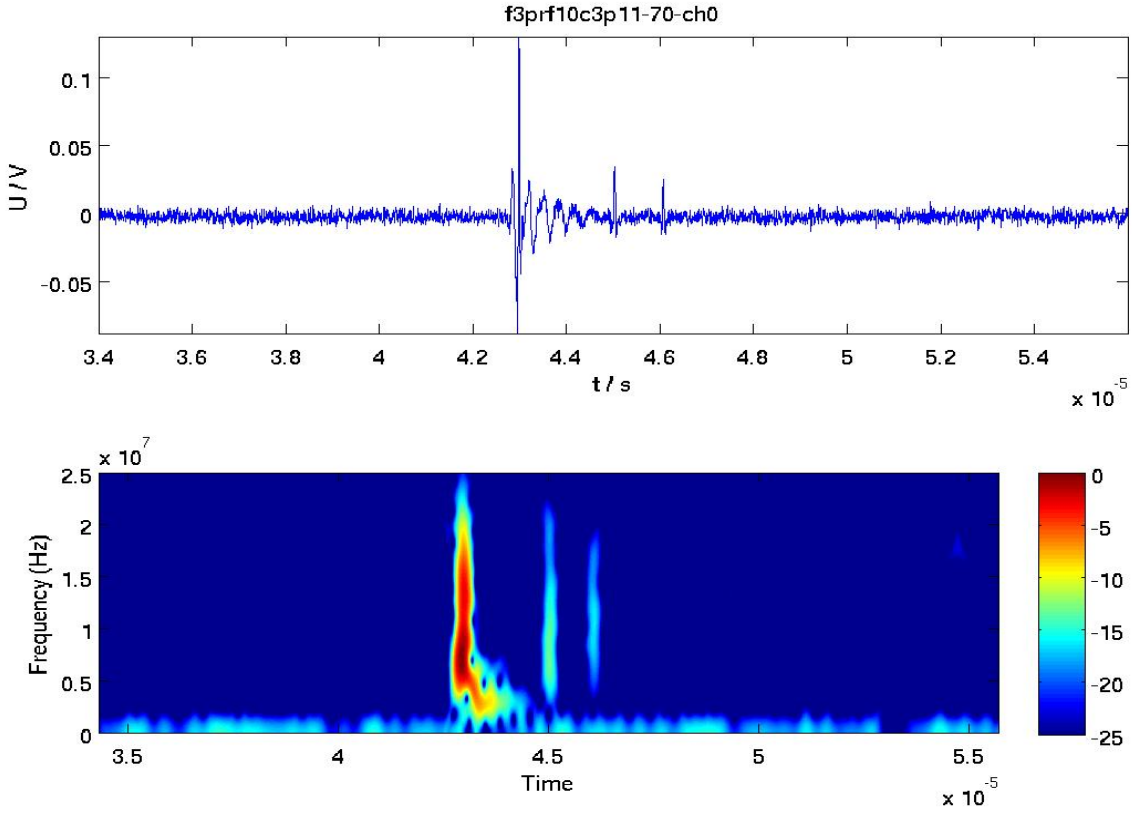

Fig 4. Representative waveform of the class "Collapse". A 2.8-MHz 3-Cycle sinusoidal tone burst was used to excite this bubble.

iv. Multiple Bubbles

Waveforms of the class Multiple Bubbles show certain characteristics of both the Oscillation and Collapse classifications. However, the PCD response contains signals of multiple microbubbles. In Fig. 5, there are two microbubble responses, The first is between 43 μs and 435 μs. The second appears between 44 μs and 46 μs. In an effort to exclude false inertial cavitation threshold statistics, the Multiple Bubble class data was not used for threshold estimation.

Fig 5. Classification of the Signal "Multiple Bubble"

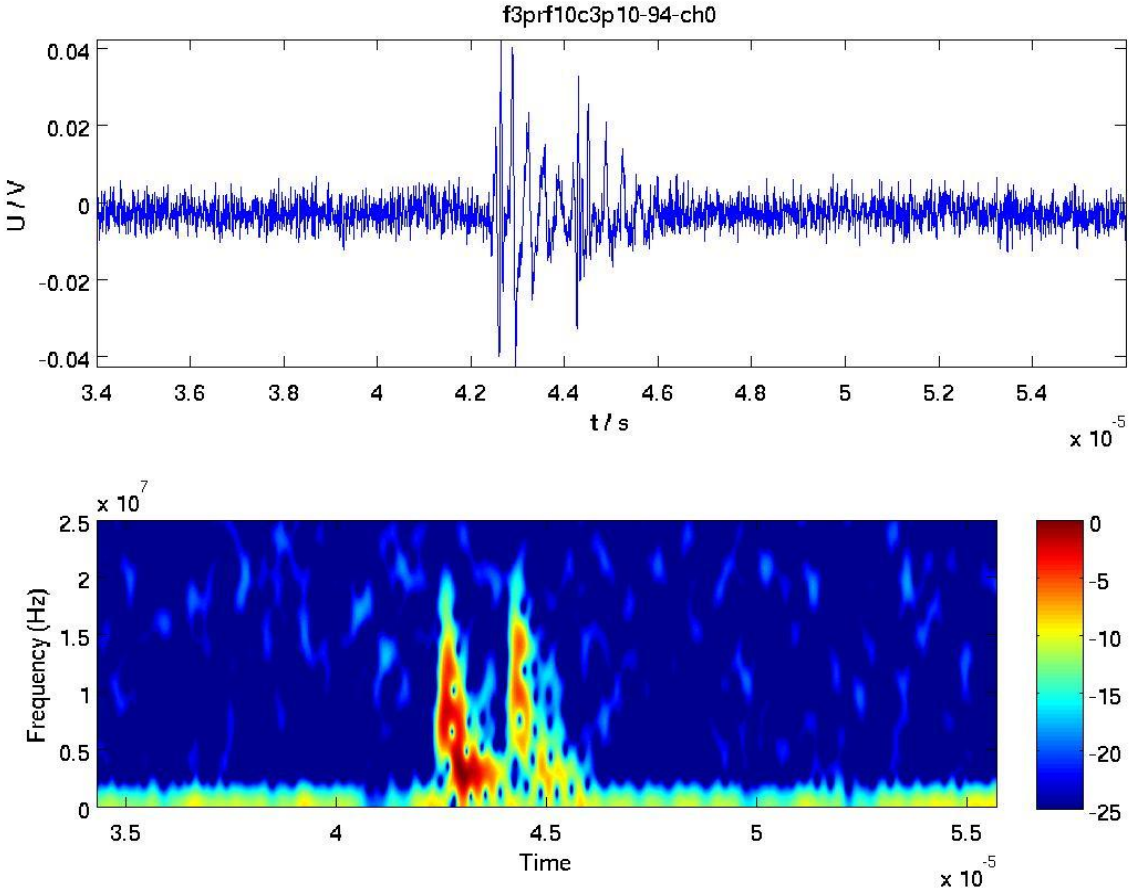

Fig 5. Representative waveform of the class "Multiple Bubbles". A 2.8-MHz 3-Cycle sinusoidal tone burst was used to excite this bubble.

v. Unidentified

All waveforms that could not be classified under Collapse, Oscillation, Noise, or Multiple Bubble were classified under the class Unidentified. This class was not factored into the inertial cavitation threshold data.

III. EXPERIMENTAL RESULTS

A. Intertial Cavitation Threshold Estimation

For all pressure levels, 500 samples were collected and a spectrogram was created from the ten highest amplitude waveforms per sample. The inertial cavitation threshold estimate was made by inspecting the data for the lowest peak rarefactional pressure where microbubble collapses were present for the contrast agent Definity®.

B. Experimental Results

After inspection of data, this study found collapse threshold estimates for all pressure levels (*0.9, 2.8, 4.6 and 7.1 MHz*; 3, 5, 7 PD) as seen in *Table* 1 and *Fig 7. Fig* 6. shows a model representative echo waveform and its time-frequency spectrogram for a single microbubble. The 2.8 *MHz, 3-cycle* PD transmit pressure waveform had a peak rarefactional pressure of 1.53 MPa. The echo waveform between approximately 450 and 470 μs corresponds to the PCD response of the microbubble in the class "collapse" due to the excitation. The postexcitiation, short-duration broadband responses correspond well to the anticipated acoustic signature due to the inertial collapse and "rebound" signals from free formed bubbles. This model was followed in determining thresholds for all pressure levels. These levels can be seen in Table 1 and can been seen graphically in Fig 7. However, this study could not determine a collapse threshold at 8 *MHz,* 7-cycle PD because there were no collapses at this pressure level.

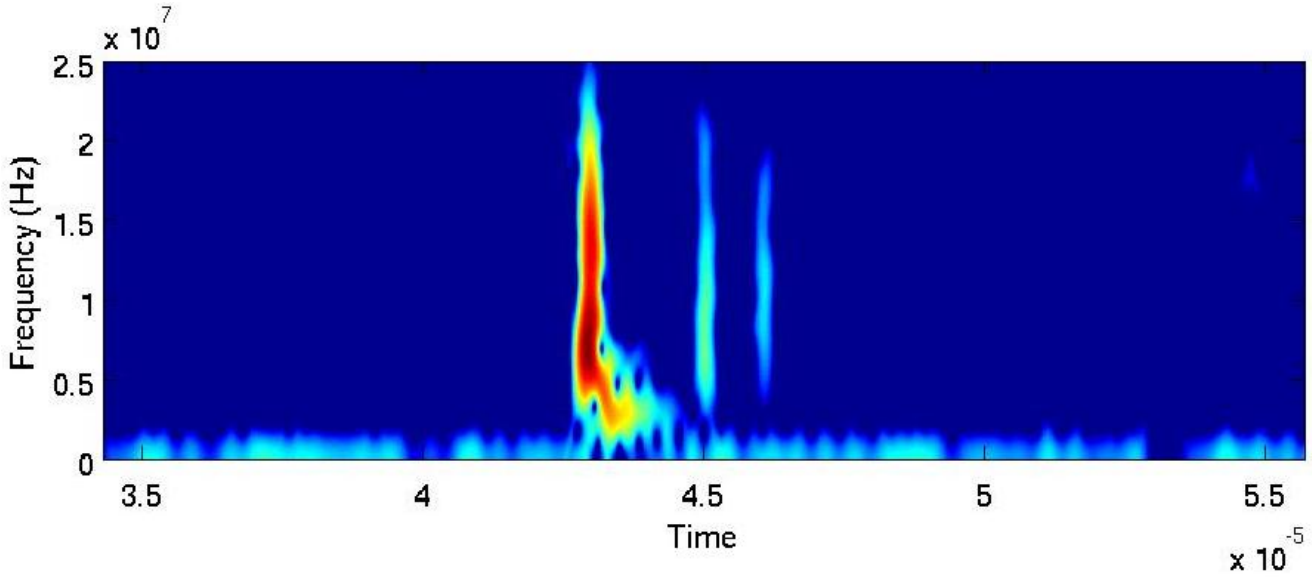

Fig 6. Model Classification of the Signal "Collapse"with a "Rebound" Criterion

Fig 6. Representative waveform of the class "Collapse". A 2.8-MHz 3-Cycle sinusoidal tone burst was used to excite this bubble.

Table 1. Estimated Peak Rarefactional Pressure Collapse Thresholds

Cycles	0.9 *MHz*	2.8 *MHz*	4.6 *MHz*	7.1 *MHz*
3	0.89 *MPa*	1.53 *MPa*	0.52 *MPa*	1.20 *MPa*
5	1.29 *MPa*	1.72 *MPa*	0.72 *MPa*	0.44 *MPa*
7	0.82 *MPa*	2.27 *MPa*	0.72 *MPa*	-

Table 1 Rarefactional pressure (MPa) estimated collapse thresholds for each transducer and pulse duration combination

Fig 7. Graphical Analysis of Estimated Peak Rarefactional Pressure Collapse Thresholds

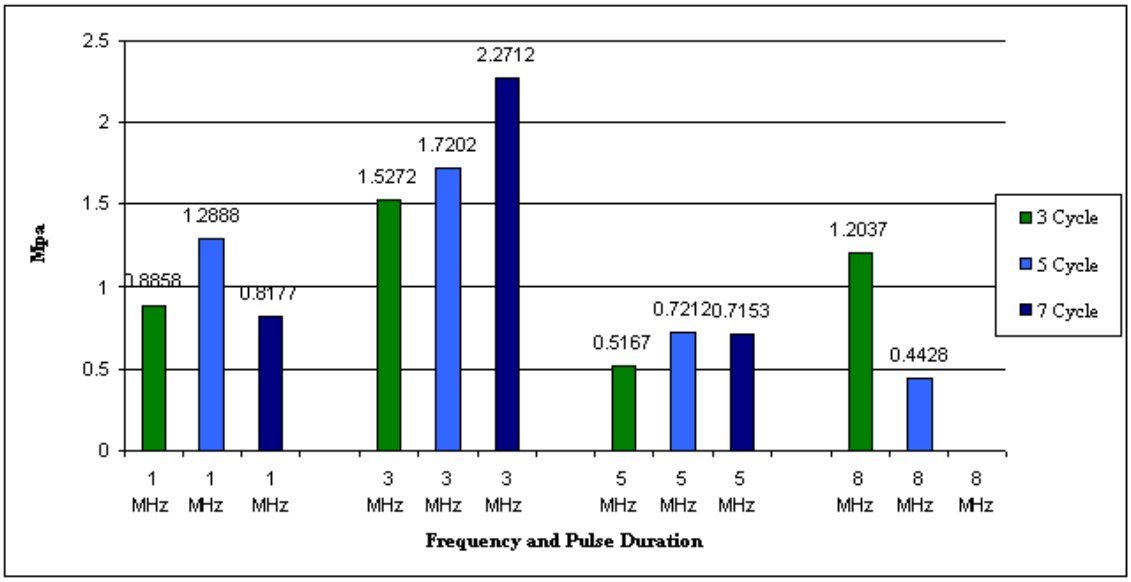

Fig. 7 Rarefactional pressure (MPa) estimated collapse thresholds for each transducer and pulse duration combination

IV. DISCUSSION

Although the cause is indefinite, observed destruction eliciting a neovascular response appears to require the interaction of US with UCAs, not does not occurr in tissues treated with US or UCAs alone. (Song et al, 2002b). Additionally, UCAs have the advantage of being strictly intra-vascular, and do not diffuse out into extra-vascular space (Ferrara et al. 2000). Knowing that all studies that have elicited a neovascular response use both UCAs and US, it is presumably safe to assert that inertial cavitation of UCAs is required to arouse a response. If this response is present, then the studies must be above the threshold for cavitation, otherwise, no result would be present if cavitation did not occur.

Several studies have produced a bruising or hemorrhaging result due to the US-UCA interaction. Chapell et al (2005) used a 1-*MHz, 0.1 ms PD* with a 0.79 peak rarefactional experimental setup using the contrast agent Dextrose Albumin. This particular study used C57BL/6-strain mice.Bruising/hemorrhaging did occur in all trials, thus indicating that the collapse threshold was

exceeded. Using the same parameters (frequency and pulse duration), our study found a .89 *MPa* collapse threshold (Fig 7.). The greater acoustic pressure level found in our study can be attributed to the lipid shell of the Definity® contrast agent as opposed to the albumin shell used by Chapell, et al. The difference between both shells is that the lipid shell of Definity® is more elastic that the albumin shell of Dextrose Albumin, thus requiring a higher pressure level to collapse the microbubble. Song et al (2002b) used a experimental setup of 1-MHz, 0.1 ms PD with a 0.79 peak rarefactional using the contrast agent Optison™. Song et al. experimented *in vivo* using rats and also targeted the *gracilis* muscle. Song et al. also found bruising/hemorrhaging in the UCA-MB group during all trials indicating that the UCA collapse threshold was exceeded. Our study again found a *.89 MPa* collapse threshold using the same parameters. The higher pressure level found in our study can be again attributed to the differences between albumin and lipid microbubble shells. Steiger et al. (2005) used a 4.4-*MHz* experimental setup with a peak rarefactional pressure of 1.1 *MPa.* This study used the lipid-shelled contrast agent MRX-815 in a rat model. Steiger et al. (2005) did not report a pulse duration, but did find bruising/hemorrhaging in all trials indicating that the UCA collapse threshold was exceeded. Using similar parameters, our study found a *.52 MPa* acoustic pressure threshold level for a 3-cycle PD, a *.72 MPa* acoustic collapse threshold level for a 5-cycle PD and a *.72 MPa* acoustic collapse threshold level for a 7-cycle PD. Since Steiger et al. did experience bruising/hemorrhaging in all trials it is presumable, according to our study, that Steiger et al. exceeded the collapse threshold by at least .3*8* MPa.

As seen in the aforementioned studies, many researchers have used albumin shelled contrast agents. However, as determined by Ammi AY, et al. (2006), the cavitation thresholds for the UCA Optison® (an albumin shelled UCA) have been recorded. In that study, Ammi, et al. determined that with a 5-cycle pulse duration at 0.9, 2.8 and 4.6 MHz the incident peak rarefractional pressures leading

to 5% microbubble rupture were 0.66, 0.83 and 1.1 MPa, respectively; and 1.1, 1.6 and 2.5 MPa for 50%. Using the same parameters, our study found a 1.29, 1.72, and .72 *MPa* collapse threshold for 5-cycle PD and 0.9, 2.8 and 4.6 *MHz* center frequencies respectively. The differences exhibited between the results of each study accentuates the differences between the less elastic albumin shelled UCAs and lipid shelled UCAs is significant and relevant and must be taken into account when considering the differences between estimated collapse thresholds.

A. Limitations

Additionally, two other factors must be considered when comparing estimated collapse thresholds. This study estimated collapse thresholds by inspecting the data for the lowest peak rarefactional pressure level at which a collapse was present. However, the weakness of this method includes the uncertainty that, if the study was be to duplicated, a lower collapse threshold may be found. Additionally, this method does not take into account the data in its entirety as opposed to a logistic regressional analysis of the data that takes advantage of all the data and determines a "best fit" line for all data sets. However, the slight weakness of using a regressional analysis is that the regression is not picking a value for a "true threshold" (the threshold at which the first collapse occurs). Instead, it is taking into account all data points meaning that collapse events could be occurring under the logistically determined collapse threshold. However, determined thresholds using the "true threshold" method (as used in this study), compared to a logistically determined threshold should, fundamentally speaking, be very similar if not equal after a sufficient amount of data is collected. Additionally, there were limitations on the data collection system (the PCD) in this study. This study questions the sensitivity of the PCD, this study speculates that the PCD is not sensitive enough due to the large variation of the signal characteristic. Furthermore, this study believes that the "rebound" criterion,

(discussed in III. EXPERIMENTAL RESULTS), used to distinguish between a collapse and a oscillation is not enough to determine the difference between both classes. This study hopes to find the acoustic signature of a single bubble that oscillates and collapses to determine other criteria, however this study has been unable to isolate a microbubble.

VI. CONCLUSION

This study experimentally determined an estimate collapse threshold for the ultrasound contrast agent Definity®. Thresholds were determined by inspecting the data for the lowest peak rarefactional pressure level at which a collapse event occurred based on a rebound criterion. This study's results were shown to be very similar to those of the literatures. Compared to Song, et al. and Chapell, et al. there was a minor difference of .10 *MPa* between their acoustic pressure level and our determined collapse threshold. In this instance, according to the difference between our threshold levels and those of Ammi, et al, the difference between the lipid shell of Definity® and the albumin shell of Dextrose Albumin and Optison™, must be taken into account. Meaning that although Song, et al. and Chapell, et al determined lower thresholds than those of this study, the differences between the UCA shells may account for the lower values. Comparing our results to those of Steiger, et al. it is apparent that our hypothesis is supported. Steiger, et al. used the MRX-815 lipid-shelled UCA, which is similar to the Definity® UCA. Although Steiger, et al. did not report a PD, it can be seen that they exceeded this study's threshold levels by at least .58 *MPa*. This difference was determined by subtracting the lowest peak rarefactional level at a 5 and 7-cycle PD (.72 *MPa)* found in this study from the 1.1 *MPa* pressure level reported in Steiger, et al. This experimentally determined information remains pertinent and necessary when considering the potential therapeutic applications due to the interaction between US

and UCAs. Although the exact mechanisms through which observed destruction eliciting a neovascular response occurs is unknown, it appears to require the interaction of US with UCAs. However, US and UCA interaction reported in Song et al. (2002a) and in similar studies such as Skyba et al. (1998) and Chapell et al. (2005), researchers elicited small capillary ruptures with application of low-frequency US to intravascular UCAs. Researchers hope that through uncharacterized wound healing mechanisms, the induced small capillary ruptures will elicit neovascularization.

A. Further Studies

This study proposes the further experimentation first and foremost regarding the potential mechanisms through with neovascularization occurs. Although it is postulated that microbubble destruction elicits this response, it is possible that thermal, shockwave or sonoporation mechanisms could affect the neovascularization response. Moreover, this study also supports the further experimentation in order to reveal an exact relationship between the degree of inflammation due to US-UCA interaction and the extent of neovascular remodeling.

VII. ACKNOWLEDGEMENTS

I would like to thank Dr. William D. O'Brien for his veteran guidance, undying support and eagerness to see me suceed. I would also like to thank Alexander Haak who took special interest in the success of this study and took much time to help. Lastly, I would like to thank the entire Bioacoustics Research Laboratory at the Universtiy of Illinois for their amazing support.

VIII. REFRENCES

[1]Assmus B, Schachinger V, Teupe C, et al. Transplantation of progenitor cells and regeneration enhancement in acute myocardial infarction (TOPCARE-AMI). Circulation 2002;106:3009 – 3017.

[2]Barnett SB, Rott HD, ter Haar GR, Ziskin MC, Maeda K: The sensitivity of biological tissue to ultrasound. Ultrasound Med Biol 1997, 23:805-12.

[3]Bekeredjian R, Chen S, Frenkel PA, Grayburn PA, Shohet RV. Ultrasound-targeted microbubble destruction can repeatedly direct highly specific plasmid expression to the heart. Circulation 2003; 108:1022–1026.

[4]Grines C, Rubanyi GM, Kleiman NS, Marrott P, Watkins MW. Angiogenic gene therapy with adenovirus 5 fibroblast growth factor-4 (Ad5FGF-4): a new option for the treatment of coronary artery disease. Am J Cardiol 2003;92:24N–31N.

[5]A. Haak and W. D. O'Brien, Jr. Detection of Microbubble Ultrasound Contrast Agent Destruction Applied to Definity®. Proceeding of the International Congress on Ultrasound, Paper Number 1719. Available at http://papers.icultrasonics.org/, 2007.

[6]A. Haak, B. Castaneda and W. D. O'Brien, Jr. Semiautomatic Detection of Microbubble Ultrasound Contrast Agent Destruction Applied to Definity® Using Support Vector Machines. Proceedings of the 2007 IEEE Ultrasonics Symposium, pp. x-x, 2007; accepted for publication.

[7]Hynynen K, McDannold N, Vykhodtseva N and Jolesz F A 2001 Noninvasive MR imaging-guided focal opening of the blood–brain barrier in rabbits Radiology 220 640–6

[8]Iba O, Matsubara H, Nozawa Y, et al. Angiogenesis by implantation of peripheral blood mononuclear cells and platelets into ischemic limbs. Circulation 2002;106:2019 –2025.

[9]Ito WD, Arras M, Winkler B, et al. Monocyte chemotactic protein-1 increases collateral and peripheral conductance after femoral artery occlusion. Circ Res 1997;80:829–837.

[10]Iwaguro H, Yamaguchi J, Kalka C, et al. Endothelial progenitor cell vascular endothelial growth factor gene transfer for vascular regeneration. Circulation 2002;105:732–738.

[11]Kaul S. Myocardial contrast echocardiography: basic principles. Prog Cardiovasc Dis 2001;44:1–11.

[12]Kondo T, Misik V, Riesz P. Effect of gas-containing microspheres and echo contrast agents on free radical formation by ultrasound. Free Radic Biol Med 1998;25:605– 612

[13]Luo H, Birnbaum Y, Fishbein M C, Peterson T M, Nagai T, Nishioka T and Siegel R J 1998 Enhancement of thrombolysis in vivo without skin and soft tissue damage by transcutaneous ultrasound Thromb. Res. 89 171–7

[14]Porter T R, LeVeen R F, Fox R, Kricsfeld A and Xie F 1996 Thrombolytic enhancement with perfluorocarbon-exposed sonicated dextrose albumin microbubbles Am. Heart J. 132 964–8

[15]Porter TR, Xie F, Kilzer K. Intravenous perfluoropropane-exposed sonicated dextrose albumin produces myocardial ultrasound contrast that correlates with coronary blood flow. J Am Soc Echocardiogr 1995;8:710 – 718.

[16]Christine Savoye, Octave Equine, Olivier Tricot, Olivier Nugue, Benoit Segrestin, Karine Sautire, Mariam Elkohen, Eduard Matei Pretorian, Kouroch Taghipour, Andre Philias et al., Left Ventricular Remodeling After Anterior Wall Acute Myocardial Infarction in Modern Clinical Practice (from the REmodelage VEntriculaire [REVE] Study Group), The American Journal of Cardiology, Volume 98, Issue 9, , 1 November 2006, Pages 1144-1149.

[17]Schirmer SH, Royen NV. Stimulation of collateral artery growth: a potential treatment for peripheral artery disease. Expert Rev Cardiovasc Ther 2004;2:581–588.

[18]Shohet RV, Chen S, Zhou YT, et al. Echocardiographic destruction of albumin microbubbles directs gene delivery to the myocardium. Circulation 2000;101:2554 –2556.

[19]Song J, Cottler PS, Klibanov AL, Kaul S, Price RJ. Microvascular remodeling and accelerated hyperemia blood flow restoration in arterially occluded skeletal muscle exposed to ultrasonic microbubble destruction. Am J Physiol Heart Circ Physiol 2004;287: H2754–H2761. Taniyama Y,

[20]Tachibana K, Hiraoka K, et al. Local delivery of plasmid DNA into rat carotid artery using ultrasound. Circulation 2002a; 105:1233–1239.

[21]Trubestein G, Engel C, Etzel F, Sobbe A, Cremer H, Stumpff U: Thrombolysis by ultrasound. Clin Sci Mol Med Suppl 1976,3:697s-698s.